INDONESIAN JOURNAL ON GEOSCIENCE
Geological Agency
Ministry of Energy and Mineral Resources

Journal homepage: http://ijog.geologi.esdm.go.id
ISSN 2355-9314, e-ISSN 2355-9306

Geochemistry of Late Triassic weak Peraluminous A-Type Karimun Granite, Karimun Regency, Riau Islands Province

Ronaldo Irzon

Centre for Geological Survey, Geological Agency, Ministry of Energy and Mineral Resources
Jln. Diponegoro No.57 Bandung, Jawa Barat, Indonesia

Corresponding author: ronaldo_irzon@yahoo.com
Manuscript received: December 01, 2015; revised: March 03, 2016;
approved: December 23, 2016; available online: January 26, 2017

Abstract - Karimun is an island with various geological deposits: tin, granite, sand, and others. The tin deposit in Karimun is related to the granitoid tin belt which extends from Myanmar to western Indonesia. Late Triassic Karimun Granite is composed of quartz, K-feldspar, plagioclase, biotite, and/or muscovite with small amounts of accessory minerals. The granitoid unit is different with other felsic intrusive rocks in Malay Peninsular because of its A-type affinity although it is classified as part of the Tin Islands. All eight samples can be classified as altered rocks since the occurrence of secondary chlorite was identifed both macroscopically and microscopically. Petrography was used to describe the minerals that form the samples, whereas XRF and ICP-MS were used to study Karimun Granite from the geochemical point of view. Harker diagrams confirm that the granites show similarity to other granite units in Malaysia except for CaO. Whalen diagrams indicate the granite as A-type as well as the SiO_2, REE, and LILE amounts. REE content in the weak peraluminous granitoid ranges from 183 to 3,296 ppm with Eu and Ce show negative anomalies in the REE spider diagram. Negative anomalies of Eu, Ba, Sr, P, and Ti in normalized spider plot also conclude that the studied granitoid indicates A-type.

Keywords: Karimun, tin belt, geochemistry, A-type, REE

How to cite this article:
Irzon, R., 2017. Geochemistry of Late Triassic weak Peraluminous A-Type Karimun Granite, Karimun Regency, Riau Islands Province. *Indonesian Journal on Geoscience*, 4 (1), p.21-37. DOI: 10.17014/ijog.4.1.21-37

Introduction

Background

The continental collision between the Sibumasu and Indochina in Malay Peninsular in latest Permian to Late Triassic period produced wide-spread magmatic activity. This collision happened after a prolonged subduction of the Devonian–Triassic Palaeo-Tethys Ocean (Sone and Metcalfe, 2008; Faure *et al*., 2014). Both intrusive and extrusive rocks were emplaced before, after, and during the collision of the paleocontinents. The development of well known three parallel belts of Southeast Asia: the Eastern Belt, the Central Belt, and the Western Belt are related to the tectonic event. These three north-south-trending zones were classified based on differences of stratigraphy, mineralization, and structure (Metcalfe, 2000). Researches were conducted to study about granitoids with relation to the tectonic pattern of Malay Peninsular. For example, granitic rocks from Endau Rompin (Ghani *et al.,* 2013) and Muncung Granite (Irzon, 2015) were emplaced due to the collision of two

blocks and are called as syn-collision granites. On the other hand, the main peak of post-collisional plutonism took place in 220-200 Ma, the period of stanniferous granites in Sumatra and Malay Peninsular were generated (Barber *et al*., 2005).

Karimun Regency of Riau Islands Province consists of three main islands: Karimun, Kundur, and Moro. Pulunggono and Cameron (1984) proposed that southwards extension of the Bentong-Raub Line traversed between the Kundur and Karimun Islands. Karimun Island is specific for containing many deposits such as tin, granite, sand, and others. The soils as the products of weathering mostly covers all the rocks, less fertile for cultivation. Karimun Granite, that is also known as Karimun Besar Granite, is considered as one of the best quality granitic rocks in the world for its content. PT. Karimun Granite is the largest company that runs the granite mining in the regency, and it began to be export the granite to Singapore in 1972 about 170,000 tons/month. Along with the end of Singkep mining, tin mining in the regency started to decline since 1991 (Diantoro, 2014). The tin deposit in Karimun is related to the granitoid tin belt which extends from Myanmar to Billiton Island. Cobbing *et al.* (1992) classified the Karimun Granite as part of the Main Range Granite Province, while Kurniawan (2014) considered it as part of the Eastern Granite Province.

This paper deals essentially with the geochemistry characteristic of the Karimun Granite: major, trace, and rare earth elements. The geochemical crarateristics are then compared to other granite intrusions in Peninsular Malaysia. The Karimun Granite has not been dated radiometrically, but Cameron *et al.* (1982) suggested a date of emplacement between Mid and Late Triassic (Carnian-Norian). Previous authors proposed that the Karimun Granit was an A-type granitoid which covered Malarco Formation by contact metamorphism (Cobbing *et al*., 1992).

Geological Setting

Geographically, Karimun Island is located in the east of Sumatra at the coordinates of 113°30' - 114°00' E and 0° 35' - 01° 10' N (Figure 1). The studied location is generally made up of hills as remnants of an erosion. The hill slopes of Karimun are normally steeper than 45% and are covered by a primary forest. The temperature range is 23.1º - 33.2ºC with humidity between 60% - 98% (Djunaedi *et al*., 2005). Tanjung Balai, located in Karimun Island, is the capital city of the Karimun Regency.

Karimun Island is included in the Geologic Map of Bengkalis Quadrangle (Cameron *et al*., 1982). Merah Complex outcrops in the southeastern area of Karimun Besar Island and principally consists of nonfoliated, variegated hornblende metagabbro. The mafic rock unit was probably emplaced in Early Devonian (Cameron *et al*., 1982). Most area of Karimun Island and other surrounding islands are occupied by granitoid. Based on the map description, the Late Triassic Karimun Granite intrudes Permian to Mid Triassic Malang/Malarco Formation. The Karimun Granite comprises biotite granites, tourmaline aplites, pegmatites, and greisens, while Malang Formation consists of hornfelsed shales, sandstones, limestones, and rhyodacitic volcanics. Quaternary deposits are distributed in Older Superficial Deposits and Younger Superficial Deposits. The Late Pleistocene Older Superficial Deposits are composed of clays, silts, and granite sand, while Holocene Young Superficial deposits comprise clays, silts, peat swamps, and coral reefs.

Field Description

Totally, eight granitoid samples were collected for this study. The studied granitoids are generally composed of quartz, K-feldspar, plagioclase, biotite, and or muscovite with small amounts of accessory minerals. Note that no hornblende can be detected macroscopically. Sample from Meral (GKR 37) was taken from an outcrop forming a hill of granite with intergrowth fractures. GKR 39 is an oxidized rock in an active iron mining area as the colour is not as bright as other samples. Just nearby the outside the mining location, another light grey granitoid outcrop was identified (GKR 58). GKR 40 and GKR 42 are granitoid boulders from Lembah Permai, which are light grey in

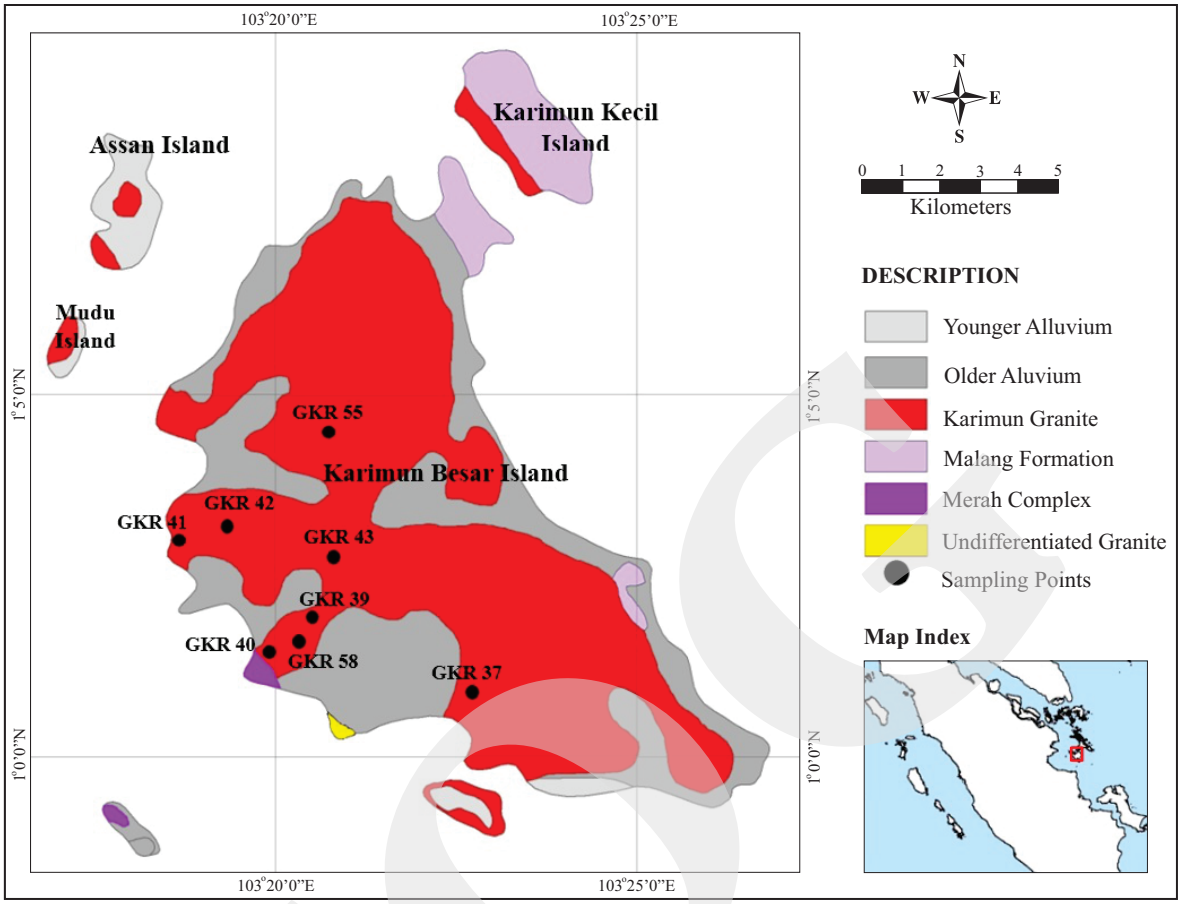

Figure 1. Geological map of Karimun Island and the sampling points (modified from Cameron *et al.,* 1982).

colour, holocrystalline-phaneritic of medium grain**.** A big size of greenish mineral, about 2 mm, in a granitoid outcrop was detected near the west coast of the island (GKR 41). Two medium grain granitoids (GKR 43 and GKR 55) located in Guntung Puna area showing oxidized layers, were taken from five meters high outcrops. Chlorite as an alteration mineral was clearly detected macroscopically in all these samples. Some field conditions are shown in Figure 2.

Analytical Method

Both petrography and geochemistry analyses were done in the geological laboratory of the Centre for Geological Survey in Bandung. The whole granitoid samples were dried at the room temperature for one day in minimum. Dried samples were then crushed with jaw crusher to gain the particle size of 200 mesh and were grounded using a ball mill. Pressed pellets were analyzed with the Advant XP X-ray fluorescence method (XRF) for the major oxides (SiO_2, TiO_2, Al_2O_3, Fe_2O_{3T}, MnO, MgO, CaO, Na_2O, K_2O, P_2O_5, SO_3) and lost of ignition (LOI). Four certified reference material pellets: STSD 1, STSD 2, STSD 3, STSD 4, and LKSD 1-4 were measured using the same procedure as the samples and were used in data calibration.

For totally 23 trace and rare earth element analyses, 100 mg of sample powder were weighted carefully, then placed in the crucible. The samples were dissolved with three acids leach: using nitric acid (HNO_3, ultrapure grade), formic acid (HF, ultrapure grade), and perchloric acid ($HClO_4$, pro analysis grade) at 120°C until all the acids were evaporated. Ultrapure grade water was used instead of normal boiled water for rinsing or downgrading acid concentration. Nitric acid was added to the digested samples and

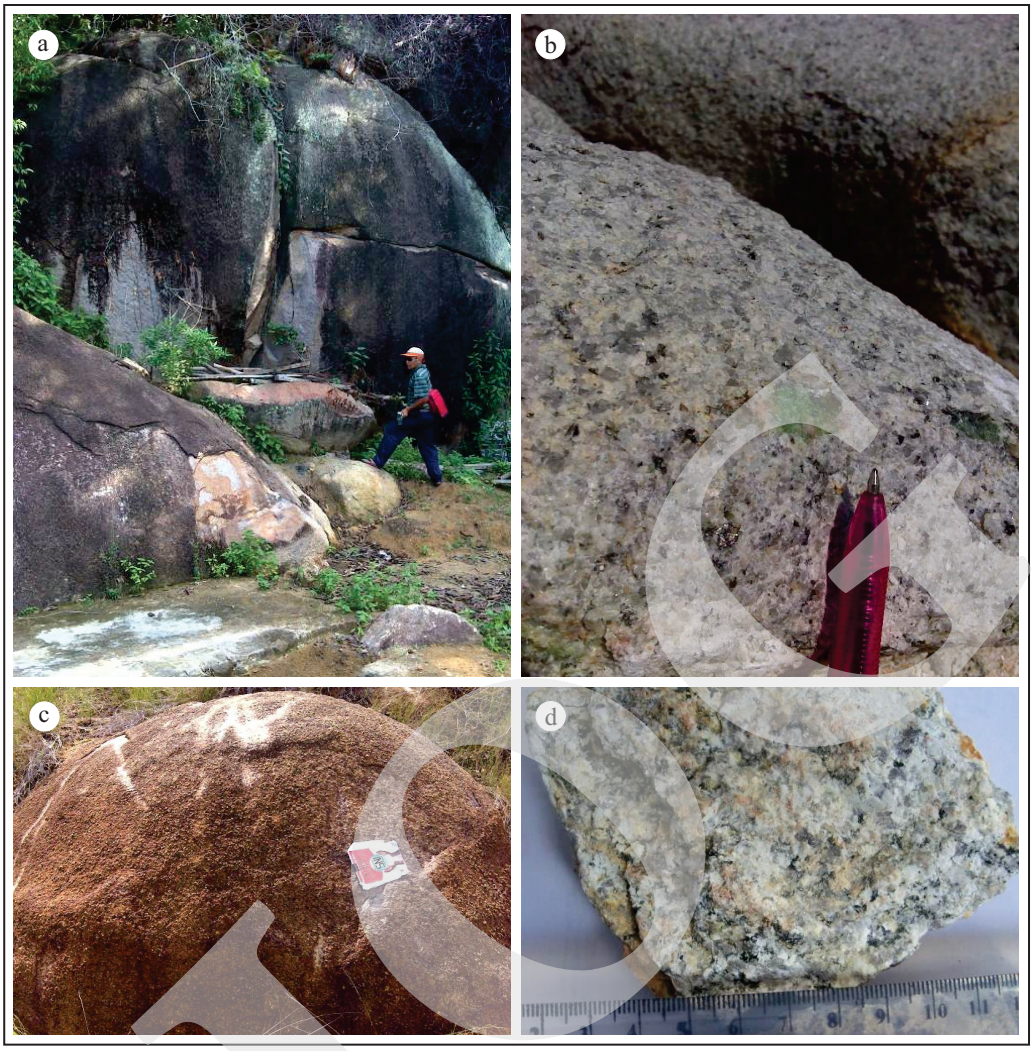

Figure 2. Field conditions of the studied samples: a) Fractures in granitoid body of GKR 37; b) A greenish mineral in GKR 41 which later was identified as chlorite in petrographic analysis ; c) Granitoid boulder of GKR 42; d) Light grey granitoid sample from a mining area in Karimun Island, GKR 39.

stored as a 'mother' solution. Few hours before ICP-MS measurement, an aliquot of the 'mother' solution was diluted with ultrapure water. GBW 7103, AGV 2, and GBW 07110 were the certified reference materials for ICP-MS analysis. Sample preparation, ICP-MS set up procedure, and certified reference evaluation are based on the study of Irzon and Permanadewi (2010).

Result and Discussion

Petrography

Megascopically, rock samples are generally light grey, holocrystalline, and medium grain granitoids. Under a microscope, the dominant minerals in decreasing abundance are quartz (22 - 45%), K-feldspar (20 - 45%), plagioclase (<25%), and biotite (<15%). Quartz crystals are anhedral, showing irregular cracks, and filling interstices among other minerals. The majority of alkali feldspar phenocrysts falls between orthoclase and sanidine series. The grain size of K-feldspars ranges from 1 to 4,3 mm. The euhedral and subhedral plagioclases may show oscillatory zoning and albite twinning as in GKR 40, GKR 43, and GKR 48. Muscovite occurs in minor amounts in GKR 39 (20%), whilst biotite as the only mafic mineral in selected samples is detected in the other seven samples. The green chlorite as biotite replace-

ment is the most abundant alteration mineral (7 - 20%). The petrographic analysis confirmed that the previous mentioned big green mineral in GKR 41 was as chlorite. The porosity of selected samples ranges from 1 to 5%. The petrographic analysis of representative samples from Karimun Granite is presented in Table 1. The modal data of petrographic analyses were then transformed into QAPF diagram of Streckeisen (1976) in Figure 3. Half of the all selected samples was classified as alkali-feldspar-granite, three samples as syeno-granite (GKR 40, GKR 43, and GKR 58), and one sample as monzo-granite (GKR 41). Microscopic pictures of some selected samples of the Karimun Granite are shown in Figure 4.

Geochemistry

Major Oxides

Chemical analyses of representative samples from Karimun Granite are given in Table 2. As felsic plutonic rocks, SiO_2 content of the studied samples is high (70.56-73.39%) and their potassic character is indicated by K_2O values which are greater than Na_2O (K_2O/Na_2O ratios >1.3). In Harker variation diagrams, TiO_2, Al_2O_3, MgO, P_2O_5, and Na_2O show descending trends *versus* SiO_2. On the other hand, K_2O, CaO, and Fe_2O_{3T} indicate positive tendencies with the silicon dioxide escalation (Figure 5). Compared to other plutons in Malay Peninsula these trends show a similarity with Boundary Range Batholith (Ahmad *et al.*, 2002), Endau Rompin Granite (Ghani *et al*., 2013), and Muncung Granite (Irzon, 2015) except for Fe_2O_{3T} and CaO *versus* SiO_2. Positive correlation of CaO to SiO_2 is unusual because the calcium oxides would decrease through magma differentiation. Plagioclase is the only Ca-bearing mineral of the selected samples. GKR 41, GKR 58, GKR 40, and GKR 43 are the four samples with plagioclase content of 25%, 15%, 13%, and 10% respectively. However, the geochemistry value does not reflect the previous petrographic data: GKR 40 (13% plagioclase) is the sample with highest CaO content (1.16%), whilst GKR 41 (25% plagioclase) only contains 0.69% of CaO. Moreover, the decrease of CaO with increasing silica in this study only shows a weak correlation coefficient with $r<<0.9$ ($r_{SiO_2\ vs.\ CaO} = 0.63$). After all, the calcium content in this study should be rechecked using different method to gain more calibrated data.

All rock samples have high alkaline (Na_2O+K_2O) contents ranging from 8.44 to 9.24%. Plots of Na_2O+K_2O *versus* SiO_2 which is known as total alkali silica (TAS) diagram (Middlemost, 1985) show that all samples lie within granite field (Figure 6a). TiO_2, MnO, MgO, and P_2O_5 are low (0.09 - 0.11%, 0.004 - 0.02%, 0.06 - 0.27%, ad 0.01 - 0.015%, respectively). Molar A/CNK ranges between 1.14 and 1.24

Table 1. Petrographic Data (vol %) of Selected Samples

	Sample	GKR 37	GKR 39	GKR 40	GKR 41	GKR 42	GKR 43	GKR 55	GKR 58
Phenocryst	Quartz	45	34	30	22	34	30	28	22
	K-Feldspar	30	22	45	20	36	32	38	32
	Plagioclase	-	-	13	25	-	10	-	15
	Hornblende	-	-	-	-	-	-	-	-
	Biotite	7	2	-	9	5	15	5	10
	Muscovite	-	20	-	-	-	-	-	-
	Opaque mineral	2	1	2	1	2	1	2	2
Accessory mineral		-	-	-	-	-	-	-	-
Alteration mineral	Sericite	2	4	-	2	5	2	6	2
	Oxydized ore mineral	2	1	-	1	2	2	2	3
	Chlorite	10	14	8	15	13	7	18	12
	Sec. quartz	-	-	-	-	-	-	-	-
Porosity		2	2	2	5	3	1	1	2

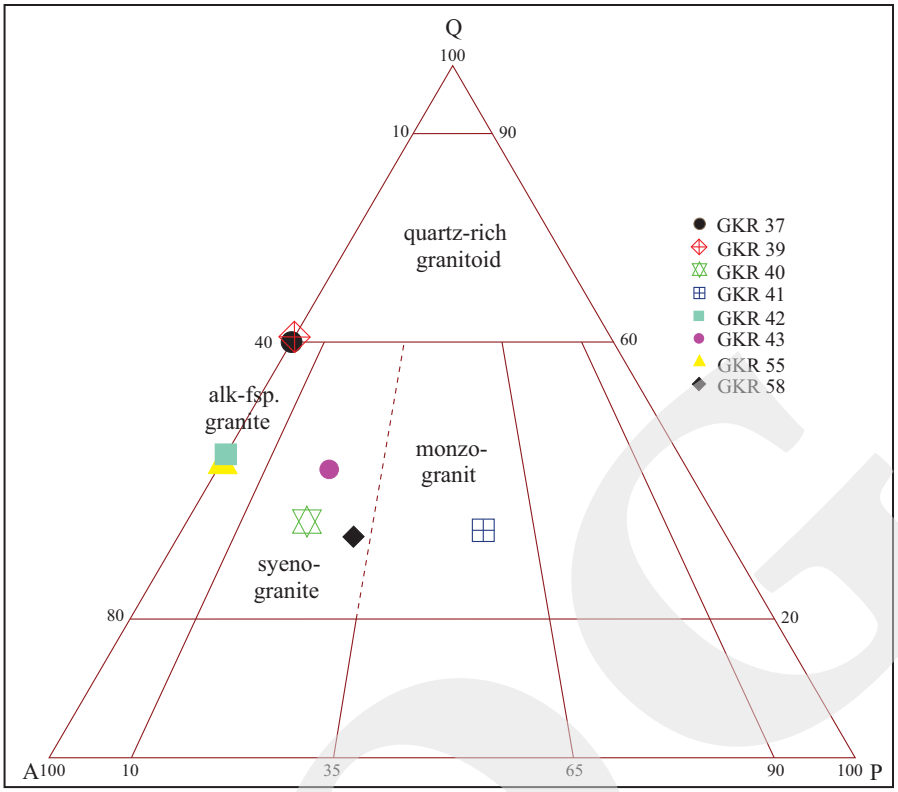

Figure 3. Normative compositions of granitoids plotted on the classification diagram of Streckeisen (1976). Q = quartz; A = Alkali feldspar; P = plagioclase.

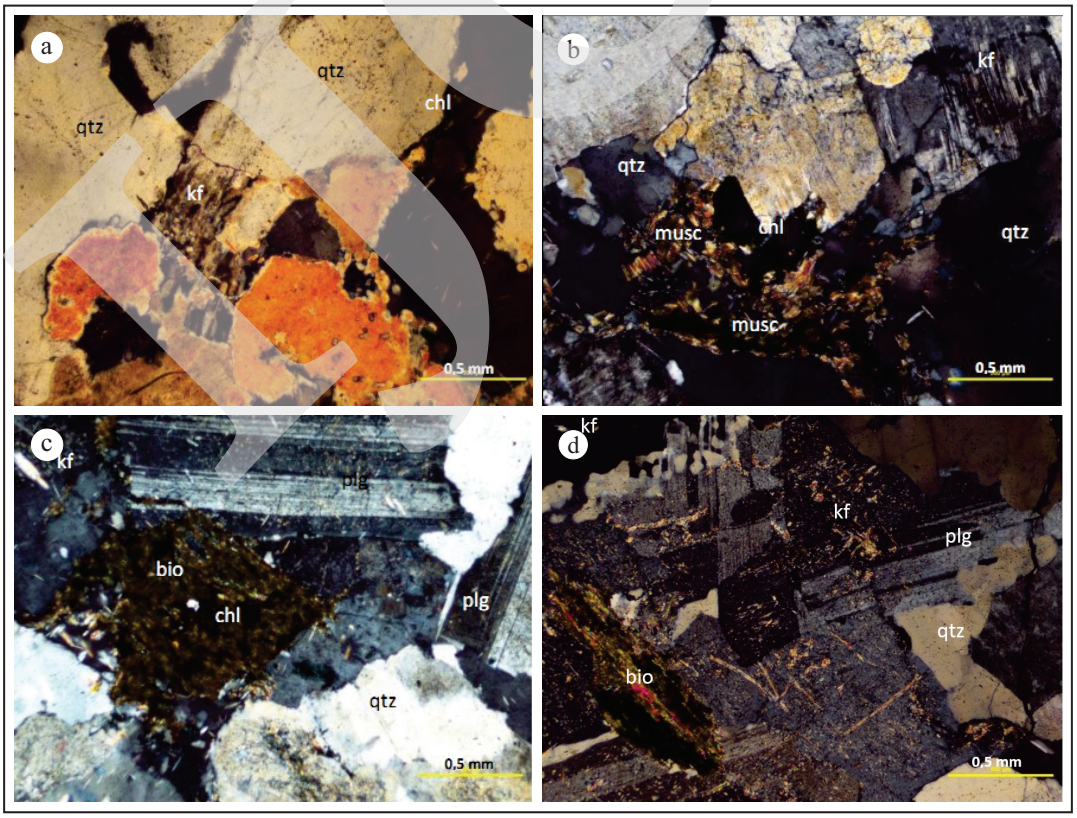

Figure 4. Photomicrographs (cross-nicols) of Karimun Granite samples. a) GKR 37; b) GKR 39; c) GKR 41; and d) GKR 58.

Table 2. Geochemistry of A-Type Karimun Granite Samples. Fe_2O_{3T}: Total Iron as Fe_2O_3

	GKR 37	GKR 39	GKR 40	GKR 41	GKR 42	GKR 43	GKR 55	GKR 58	Primitive Mantle value*
Major oxides (%)									
SiO_2	72.41	70.56	73.39	71.18	72.12	72.67	71.42	71.77	Si = 10.65
TiO_2	0.106	0.124	0.05	0.114	0.12	0.0942	0.109	0.101	Ti = 0.044
Al_2O_3	15.37	16.3	14.49	15.79	15.71	15.15	15.83	15.95	Al = 0.86
Fe_2O_{3T}	1.33	0.913	1.29	1.23	1.06	1.38	1.44	1.17	Fe = 18.1
MnO	0.0156	0.0045	0.02	0.0122	0.0065	0.0167	0.0176	0.0121	Mn = 0.192
CaO	0.6	0.542	1.16	0.697	0.788	0.794	0.74	0.721	Ca = 0.925
MgO	0.153	0.316	0.06	0.269	0.206	0.157	0.163	0.226	Mg = 9.65
Na_2O	3.87	4.04	2.75	3.89	4.13	3.72	3.93	3.75	Na = 0.51
K_2O	5.2	5.05	5.69	5.32	5.11	5.14	5.18	5.37	K = 0.055
P_2O_5	0.0121	0.017	0.01	0.0128	0.0147	0.0122	0.0127	0.014	P = 0.108
LOI	0.53	0.8	0.6	0.85	0.55	0.56	0.63	0.67	
Total	99.61	99.68	99.51	99.44	99.63	99.60	99.49	99.57	
Trace and rare earth elements (ppm)									
Sc	1.47	0.89	1.02	1.32	0.86	1.07	n.a.	n.a.	21
V	6.25	7.76	10.16	7.45	7.47	5.33	6.70	6.94	56
Ga	18.77	27.10	17.95	16.18	18.07	13.91	16.49	16.11	9.2
Rb	323.46	293.69	298.94	320.42	254.46	238.44	310.98	264.35	2.3
Sr	26.94	44.02	42.72	26.66	43.49	17.96	19.92	20.67	7.25
Y	60.69	654.64	124.75	73.78	58.07	63.18	64.17	116.29	1.57
Nb	1.67	2.35	1.20	2.12	2.64	0.74	8.81	4.49	0.24
Cs	10.64	16.15	16.58	6.78	4.23	9.14	11.85	5.90	0.19
Ba	88.08	138.83	116.87	45.93	107.53	53.61	61.91	75.94	2.41
La	46.16	812.17	44.96	42.62	43.52	36.23	43.04	63.93	0.237
Ce	75.20	1105	90.36	64.64	70.09	57.32	71.39	95.08	0.613
Pr	11.49	180.47	14.44	9.91	10.43	8.71	11.15	21.65	0.0928
Nd	38.56	618.42	56.65	35.34	37.88	31.41	41.37	82.13	0.457
Sm	11.50	205.87	17.45	9.60	10.03	8.48	11.90	23.48	0.148
Eu	0.14	3.80	0.39	0.12	0.19	0.09	0.13	0.26	0.0563
Gd	10.02	141.93	17.69	9.70	9.00	7.78	10.71	21.08	0.199
Tb	2.00	21.67	3.83	2.05	1.83	1.64	2.24	4.25	0.0361
Dy	13.00	108.20	26.08	14.03	12.10	11.65	15.18	27.57	0.246
Ho	2.71	17.51	5.59	3.06	2.58	2.58	3.21	5.73	0.0546
Er	6.87	35.07	14.09	8.04	6.57	6.95	8.18	14.61	0.16
Tm	1.21	5.84	2.48	1.51	1.18	1.26	1.48	2.65	0.0247
Yb	7.72	36.12	15.11	9.76	7.48	8.33	9.45	17.25	0.161
Lu	1.09	4.59	2.12	1.44	1.07	1.19	1.35	2.44	0.0246
Tl	1.94	1.75	1.85	1.83	1.51	1.40	2.16	1.82	0.14
Th	40.03	35.90	33.84	40.03	38.83	28.98	45.34	42.26	0.029
U	14.66	15.39	13.00	19.61	15.27	11.72	16.77	16.94	0.0074
Total REE	227.67	3,296	311.26	211.82	213.94	183.64	230.79	382.09	

Fe_2O_{3T}: Total Iron as Fe_2O_3.

*(McDonough and Sun, 1995)

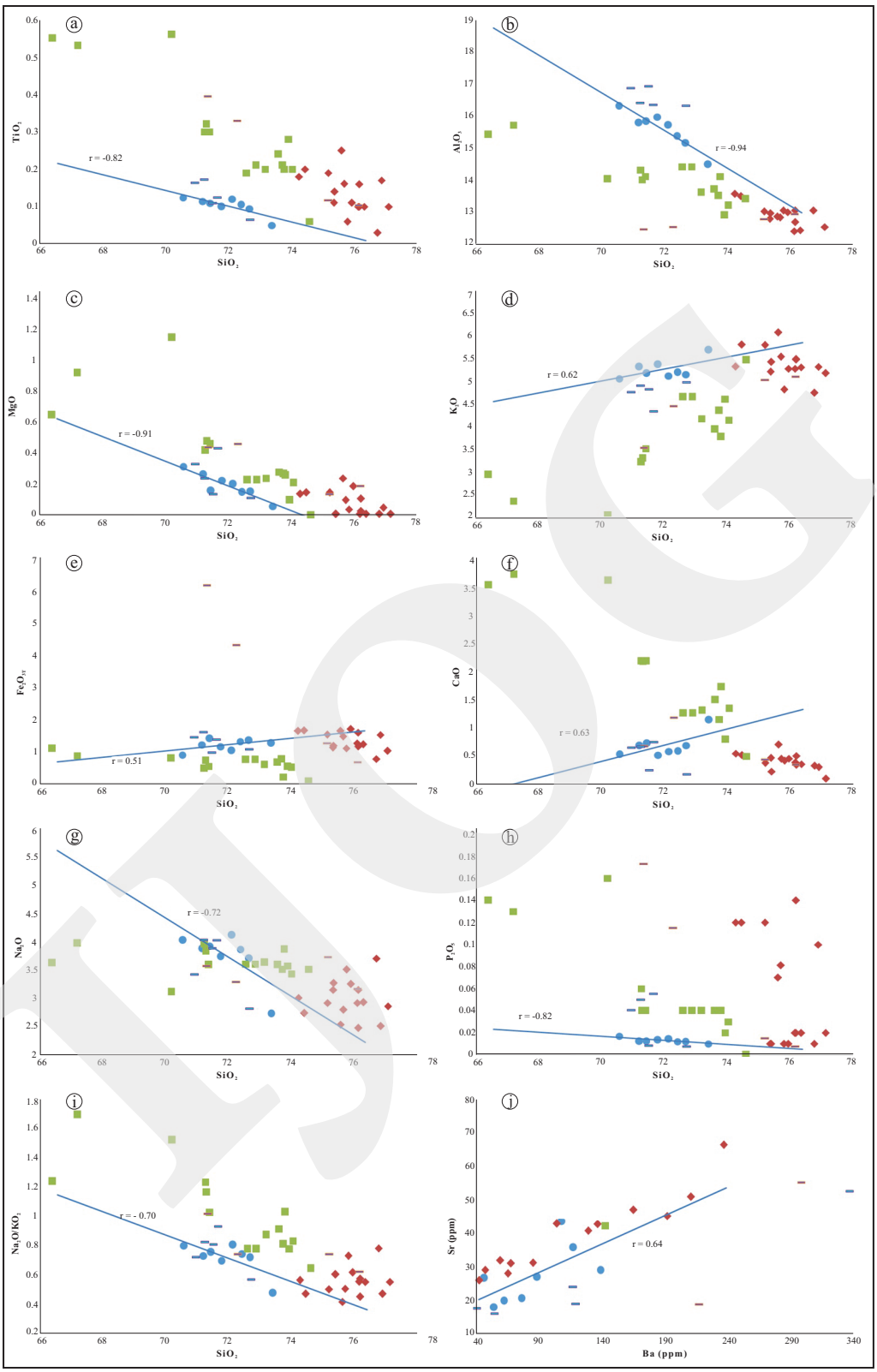

Figure 5. Binary plots of major elements in this study and other granitoid units in Malay Peninsular with their trendlines. r is the correlation coefficient for Karimun Granite samples. a) SiO_2 *vs.* TiO_2, r = -0.82; b) SiO_2 *vs.* Al_2O_3, r = -0.94; c) SiO_2 *vs.* MgO, r = -0.91; d) SiO_2 *vs.* K_2O, r = 0.62; e) SiO_2 *vs.* Fe_2O_{3T}, r = 0.51; f) SiO_2 *vs.* CaO, r = 0.63 ; g) SiO_2 *vs.* Na_2O, r = -0.72; h) SiO_2 *vs.* P_2O_5, r = -0.82; i) SiO_2 *vs.* Na_2O/K_2O, r = -0.70; and j) Ba *vs.* Sr, r = 0.64. ● = Karimun Granite, ◆ = Selim Granite (Ghani, 2005), ■ = Endau Rompin Granite (Ghani *et al.*, 2013), ▬ = Lingga Group of Muncung Granite, and ▬ = Singkep Group of Muncung Granite (Irzon, 2015).

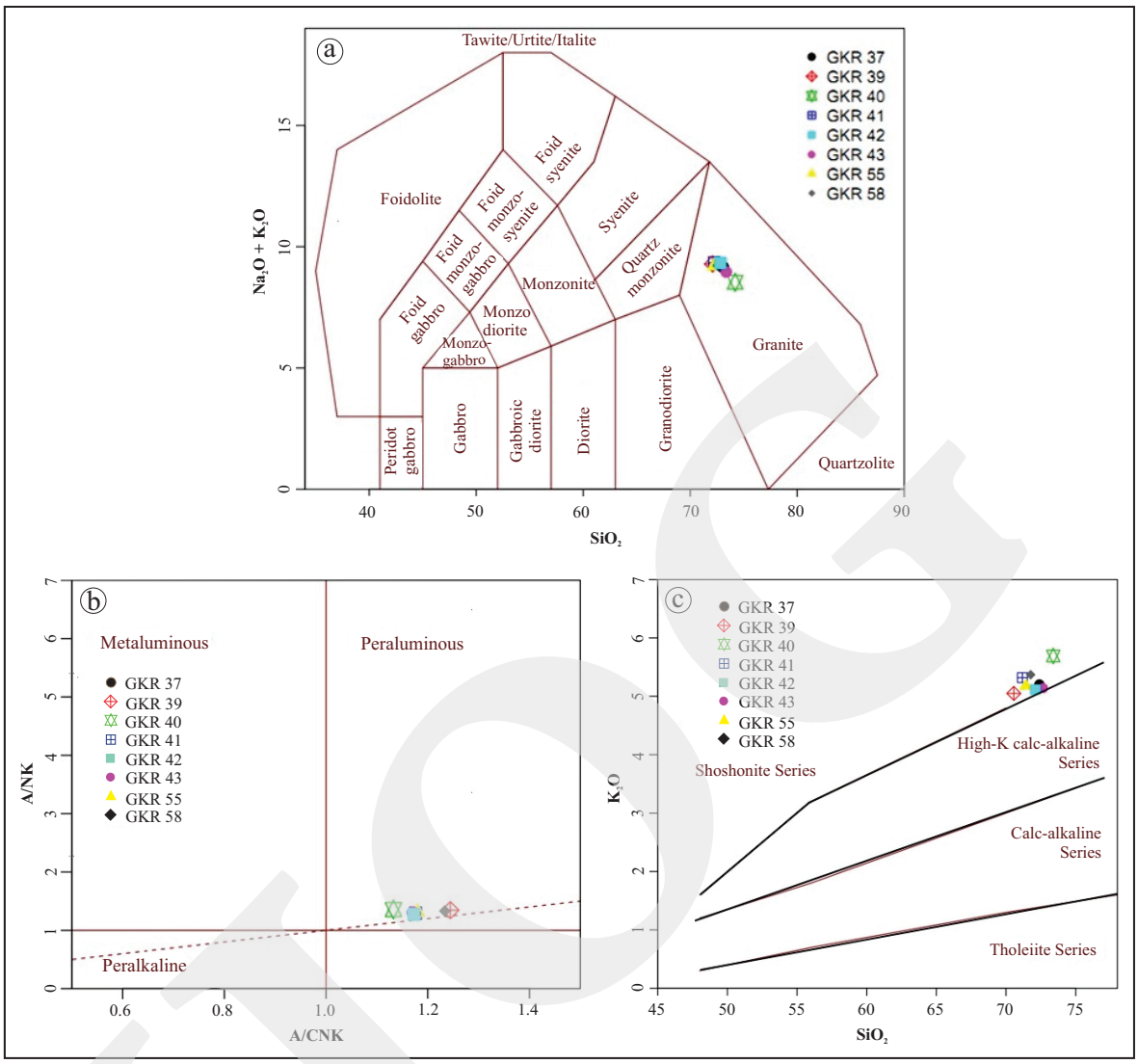

Figure 6. a) All granitoid samples from Karimun Island are classified as granite using TAS diagram of Middlemost (1985); b) A/NK *vs.* A/CNK plot, for the Karimun Granite (Shand, 1943); c) shoshonite character of studied samples (Peccerilo and Taylor, 1976).

suggesting weak peraluminous character (Figure 6b). Moreover, Karimun Granite plots in the shoshonite field with high abundances of both K_2O and SiO_2 (Figure 6c).

The 10,000×Ga/Al ratios in the Karimun Granite are 1.73 to 3.14, with the average value of 2.18. Although the average value is relatively below the global average of 3.75 for A-type granites (Whalen *et al.,* 1987), the samples fall into the A-type granite field in 10,000×Ga/Al vs. Na_2O+K_2O, $(Na_2O+K_2O)/CaO$ and K_2O/MgO diagrams (Figure 7). The diagrams agree with the previous author conclusions that A-type granites have also been identified in some of Tin Islands such as Karimun (Cobing *et al*., 1992; Barber *et al*., 2005). The Karimun Granite contains high SiO_2 (>68%) and total alkaline as another major oxide character of A-type granitoid (Christiansen and Keith, 1996; Kebede *et al*., 1999; Ahmad and Chaudhry, 2008).

Trace and rare earth elements

Fractional crystalization in magma can be observed based on trace and/or rare earth element ratios. Ba/Sr ratio ranges from 1.72 to 3.67 (2.89 in average) whereas Rb/Sr with significant variation from 5.85 to 13.28 (10.65 on the average). High Rb/Sr, Ba/Sr ratios, high K% suggest that the Karimun Granite is primarily derived from a

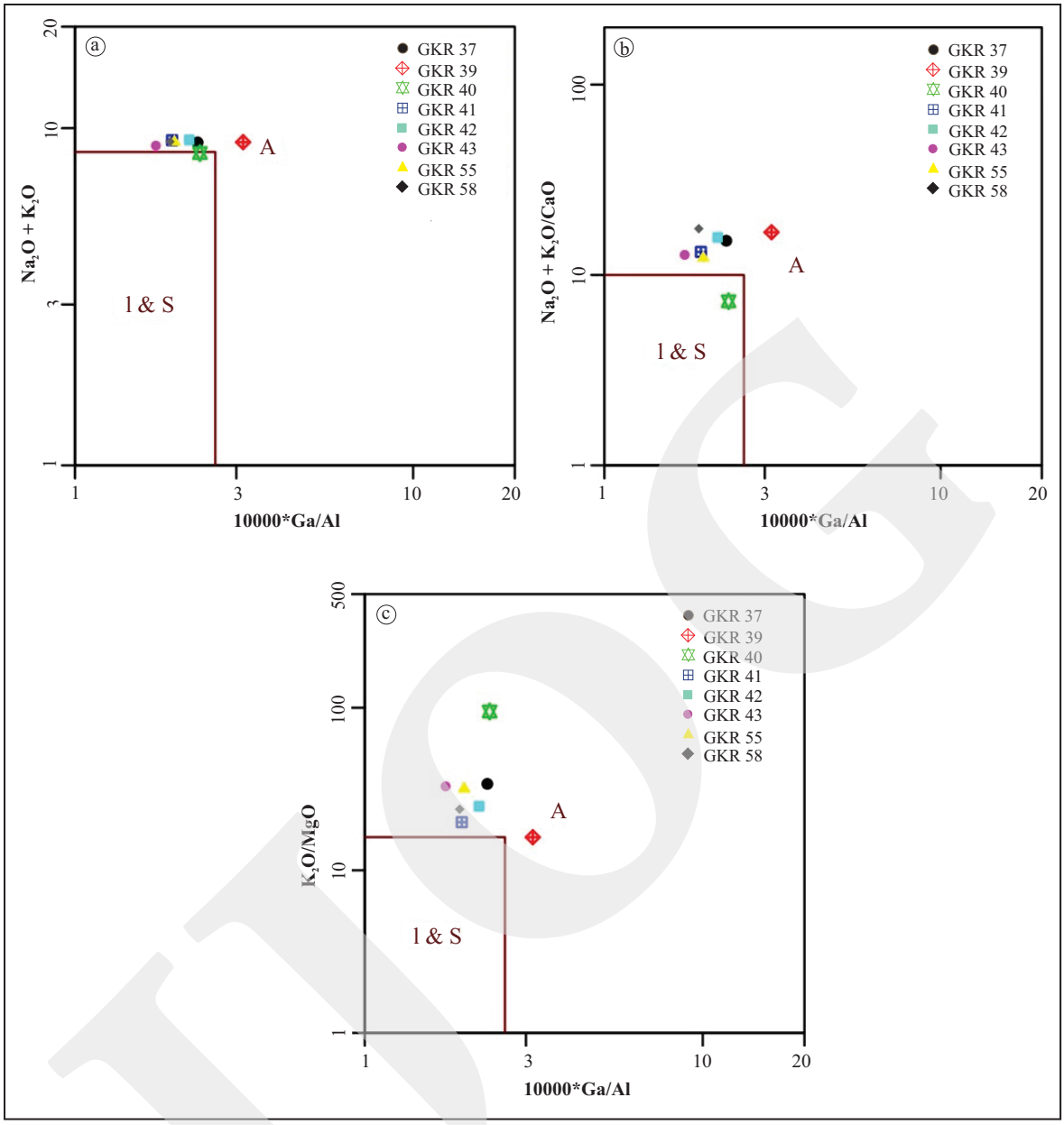

Figure 7. 10,000 Ga/Al vs a) $Na_2O + K_2O$; b) $(Na_2+K_2O)/CaO$; c)K_2O/MgO (Whalen *et al*., 1987). I = I-type granite, S = S-type granite, and A = A-type granite. Please note that the three diagrams require Ga content in samples which is not provided in previous the studies of Selim Granite (Ghani, 2005), Endau Rompin Granite (Ghani *et al*., 2013), and Muncung Granite (Irzon, 2015).

felsic source (Ray *et al*., 2011). On Ba *versus* Sr diagram, the positive correlation between Ba and Sr (Figure 5i) suggests that K-feldspar, biotite, and plagioclase are being removed in the granite differentiation (Ghani, 2005). Compared to the other granitoid units in Malay Peninsular, Rb/Sr value of the samples (5.85 - 15,61) is higher than Endau Rompin Granite (Johor - Malaysia) and both groups of Muncung Granite (Lingga Regency - Indonesia), but lower than fine- and coarse-grained Selim Granite (Perak - Malaysia) (Ghani, 2005; Ghani *et al*., 2013; Irzon, 2015) (Tabel 3). The intermediate maturity of Karimun Granite as a granitoid unit in Peninsular Malaysia is confirmed from this Rb/Sr ratio that indicates a medium to high differentiation level. Moreover, the high Rb/Sr (>2.6) and low Sr/Ba (<0.4) ratios for most of the granitoid samples (Table 3) are

consistent with plagioclase fractionation (Nagudi, 2003).

Chemically, transition elements are described as elements in the d-block of the periodic table. The group is different from other elements because that in a given inner orbital, it has less than a full quota of electrons which cause the formation in many oxydation states (White, 2013). The amount of some transition elements: Sc, V, and Nb of the studied samples are categorized low at up to 1.4, 5.3 - 10.1, and 0.7 - 8.8 ppm respectively. Contrastively, other transition elements are high: Y (53-654 ppm), Th (29 - 45 ppm), and U (11 - 19 ppm). REEs are classified as transition elements. These samples contain moderate to high and variable REE concentration of 183

Table 3. Average Major Oxides and Trace Elements Value, and Rb/Sr and Sr/Ba Ratios of Studied Samples compared to Some Other Granitoid Units in Peninsular Malaysia. Data sources: (1) Ghani (2005); (2) Ghani *et al*. (2013); (3) Irzon (2015)

	Selim Granite[1]		Endau Rompin Granit[2]	Muncung Granite[3]		Karimun Granite
	Fine grained	Coarse grained		Group A	Group B	
Major oxides (%)						
SiO_2	76.06	75.70	72.10	71.62	73.75	71.94
TiO_2	0.09	0.16	0.29	0.13	0.24	0.10
Al_2O_3	12.89	12.82	14.05	16.55	12.67	15.57
Fe_2O_{3T}	1.17	1.49	2.17	1.31	3.12	1.23
MnO	0.04	0.04	0.05	0.03	0.04	0.01
CaO	0.34	0.45	1.90	0.50	0.67	0.69
MgO	0.05	0.10	0.39	0.25	0.31	0.19
Na_2O	3.30	2.81	3.63	3.64	3.45	3.76
K_2O	5.10	5.53	3.81	4.75	4.52	5.26
P_2O_5	0.01	0.08	0.06	0.03	0.08	0.01
Trace and rare earth elements (ppm)						
Ba	46.82	136.56	958.47	167.10	440.44	86.09
Rb	756.33	610.11	167.63	280.43	175.27	288.09
Sr	25.63	42.63	167.17	25.73	62.11	27.55
Th	39.22	44.8	18.08	29.90	27.56	38.15
V	8.08	9.07	19.37	14.16	15.52	7.26
Sc	5.52	5.52	-	2.92	8.89	0.83
La	45.15	40.90	42.78	30.28	242.39	141.58
Ce	111.33	93.48	72.63	62.12	146.37	203.65
Pr	12.97	23.71	8.39	7.58	48.72	33.53
Nd	45.37	37.57	30.15	28.12	181.19	117.72
Sm	11.47	8.58	5.63	6.93	36.26	37.29
Eu	0.12	0.30	1.27	0.21	2.08	0.64
Gd	11.05	8.23	5.40	6.11	32.52	28.49
Tb	2.26	1.56	0.91	1.09	3.77	4.94
Dy	16.20	11.00	5.37	7.06	18.77	28.48
Ho	3.57	2.37	1.18	1.50	3.28	5.37
Er	10.58	6.46	3.51	4.27	8.39	12.55
Tm	1.63	1.06	0.54	0.66	1.15	2.20
Yb	10.87	6.81	3.69	4.44	7.16	13.90
Lu	1.55	0.97	0.57	0.67	1.03	1.91
∑REE	284.10	243.00	182.02	161.05	733.07	632.24
Rb/Sr	29.51	14.31	1.00	10.90	2.82	10.46
Sr/Ba	0.55	0.31	0.17	0.15	0.14	0.32

to 3,296 ppm, 632 ppm on the average (Table 2). The high amount of REE exhibits the A-type granite character (Whalen *et al.,* 1987; Goodge and Vervoot, 2006; Shellnutt and Zhou, 2007; Singh and Vallinayagam, 2012).

Primitive Mantle value of McDonough and Sun (1995) is used to normalized both trace and rare earth elements data of this study. The normalized REE patterns relatively show a stronger fractionation of light rare earth elements (LREE) ($1.70<(La/Sm)_N<2.77$) than that of heavy rare earth elements (HREE) ($0.75<(Ga/Yb)_N<3.1$) (Figure 8a). It has been observed that granitic rocks contain higher amounts of Th, U, and light rare earth elements (REEs) compared to other igneous rocks such as basalt and andesite (Sahoo *et al.,* 2011) that can explain the Th and U amounts and REE pattern of these samples. Europium and cerium negative anomalies were detected: Eu/Eu* of 0.034 to 0.068 and Ce/Ce* of 0.62 to 0.85. Both anomalies are used as indicators of magma evolution. The pronounced negative Eu anomaly may be correlated to plagioclase remaining in the source after partial melting generating the granite, where as cerium negative anomaly probably due to high oxygen fugacity at the source of the magma that cause some of trivalent ceriums were oxydized to tetravalent cerium (Salem *et al.,* 2001; Jurvanen *et al*., 2005; Papangelakis and Moldoveanu, 2014). Compared to four granitoid units in Malay Peninsular, the average total REE value of Karimun Granite is just smaller than Lingga Granite (Figure 8b). The biggest negative Eu anomaly of the group is shown by Karimun Granite whilst Endau Rompin Granite by the smallest anomaly.

A group of elements that is unsuitable in size and/or charge to the cation sites of the minerals is called incompatible element. The partition coefficient between rock-forming minerals and liquid phases of this group is much smaller than 1. This group is then divided into two subgroups: large-ion lithophile elements (LILE) and high field strength elements (HFSE). K, Rb, Cs, Sr, Ba, U, Th are elements having large ionic radius well known as LILE. On the other hand, HFSE is a group of elements of large ionic valences or high charges: Zr, Nb, Hf, Ta, Sc, Y, and the REE. The selected granitoid samples show high level of LILE at 4,643 – 5,256 ppm on the average of 4,846 ppm. This high LILE content and previous high alkali character of Karimun Granite fit the statement that A type granitoid may represent products of mantle-derived magmas with or without crustal contamination through extensive fractional crystalization, common contemporaneity with mafic syenite plutons and characterized by high alkali, LILE, and HFSE contents (Goodge and Vervoot, 2006; Dwivedi *et al*., 2011).

On a primitive mantle normalized (McDonough and Sun, 1995) extended spider diagram, the granitoid shows positive anomalies of U, La, Nd, Dy and negative anomalies of Ba, Ce, Sr, P, Y, and Ti (Figure 9). The anomalies indicate fractionation by mineral phases containing these elements at some stage in the history of the source of the magma. As Eu negative anomaly, both Ba and Sr depletions can be related to the fractionation feldspar, especially plagioclase, in the magma chamber (Mao *et al*., 2011; Keshavarzi *et al*., 2014). Fractionation of plagioclase would increase NK/A molar $(Na_2O + K_2O)/Al_2O_3$) ratios and negative Sr-Eu anomalies, while separation of K-feldspar would lead to increasing Na_2O/K_2O ratios and negative Eu-Ba anomalies. Furthermore, fractionation of K-feldspar usually follows that of plagioclase (Zhang *et al*., 2012). Selected granitoid samples display negative anomalies of Eu, Ba, and Sr (Figure 8 and Figure 9), while Na_2O/K_2O ratios decrease with increasing SiO_2 (Figure 2j), which favours fractional crystallization of both plagioclase and K-feldspar. Other authors also conclude that the negative anomalies shown by Eu, Ba, Sr, P, and Ti are typical of A-type granitoids (Ahmad and Chaudhry, 2008; Tong *et al*., 2012; Zhang *et al*., 2012). Negative Ti anomaly can be interpreted as reflecting ilmenite fractionation. The sharp negative Nb anomaly suggests that the granite melts originated from partial melting of subduction zone environment

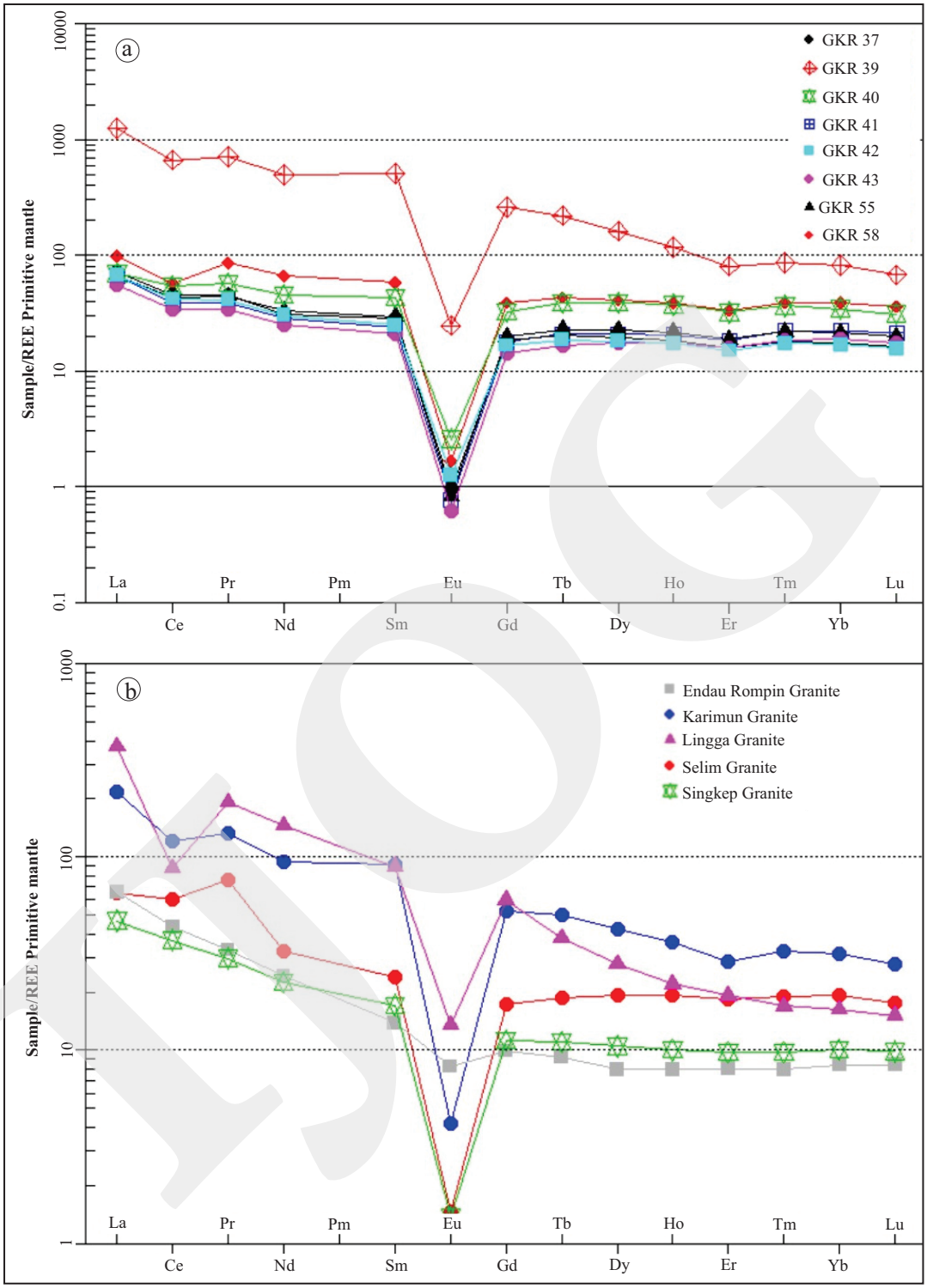

Figure 8. a) REE spider diagram of Karimun Granit samples; b) The average REE spider diagram of five granitoid units in Malay Peninsular. All values were normalized to primitive mantle value of McDonough and Sun (1995).

(Tong *et al*., 2012). On the other hand, positive anomalies would indicate element accumulation or minor fractionation of mineral related elements in differentiaton process.

Conclusions

Karimun Granites are composed mainly of quartz, K-feldspar, plagioclase, and biotite. A

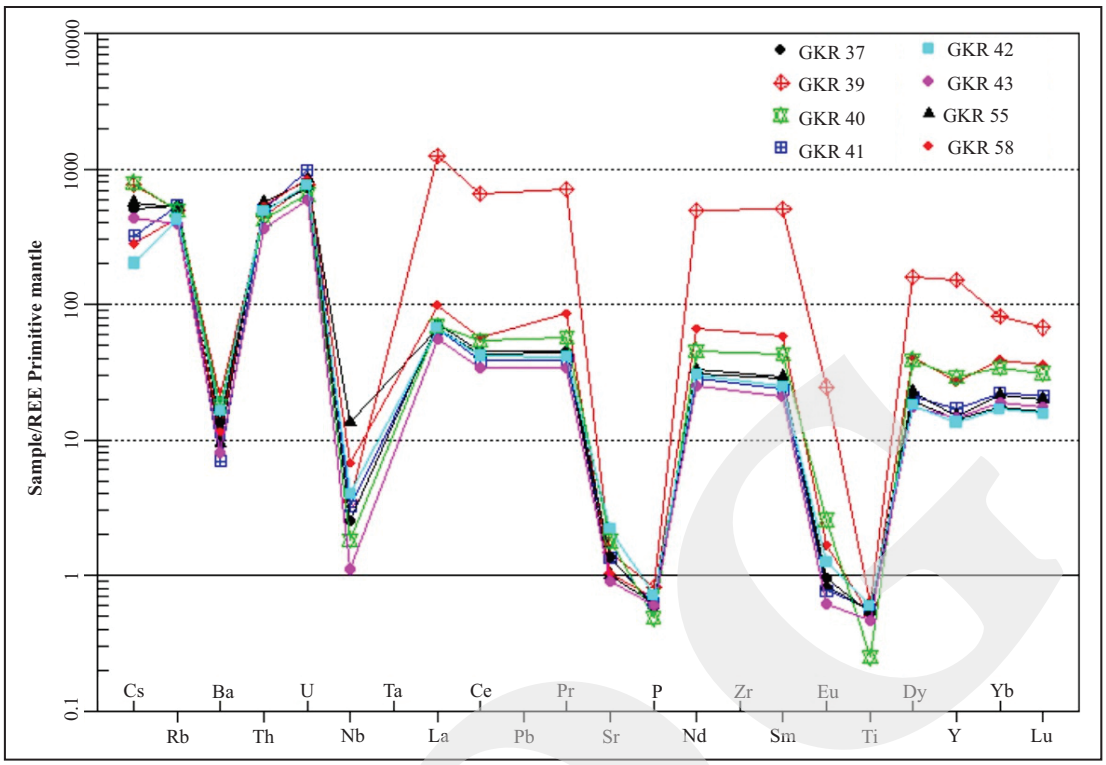

Figure 9. Extended spider-diagram of the studied samples normalized to primitive mantle. Normalization values from Sun and McDonough (1995).

number of chlorites in the eight samples indicates that the granitoids were altered. The modal data of petrography analyses classified most of the samples as alkali-feldspar-granite. TiO_2, Al_2O_3, MgO, and Na_2O show a negative corelation with SiO_2. On the other hand, K_2O increases with increasing SiO_2. The molar A/CNK suggests the weak peraluminous character, whereas high abundances of both K_2O and SiO_2 as shoshonite granitoid. Whalen diagrams and Eu, Ba, Sr, P, Ti negative anomalies concluded the A-type of Karimun Granite and agreed with the previous author conclusions that A-type granites have also been identified in some of Tin Islands. The intermediate maturity of the studied granite is confirmed from the Rb/Sr ratio. REE content of the samples ranges from 183 to 3,296 ppm, 632 ppm on the average, with stronger fractionation of LREE than HREE. Europium and cerium negative anomalies were 0.034 to 0.068 and 0.62 to 0.85, respectively. Ba, Sr, and Eu anomalies in extended spider diagram reveal the feldspar fractionation during a differentiation process.

Acknowledgements

The author is thankful to his big family for the spirit. The writer would like to thank the Head of the Centre for Geological Survey for the publicity permission. Professor Hamdan Zainal Abidin supports this paper from his scientific ideas. The very good laboratory work that was performed by Indah and Citra is highly acknowledged. Mr. Eko Partoyo, Mr. Baharuddin, and Mr. Purnama Sendjaja support the research in petrology view. Geochemistry Programme of the Centre for Geological Survey assists this research financially.

References

Ahmad, R.A., Yusoff, I., and Ghani, A.A., 2002. Geochemical characteristics of the granitic rocks from Boundary Range Batholith, Peninsular Malaysia. *Geological Society of Malaysia Annual Geological Conference*, Kelantan, Malaysia, p.243-246.

Ahmad, S.A. and Chaudhry, M.N., 2008. A-type Granites from the Nagarparkar Complex, Pakistan: Geochemistry and Origin. *Geology Bulletin of Punjab University*, 43, p.69-81.

Barber, A.J., Crow, M.J., and Milsom, J.S. (Eds.), 2005. Sumatra Geology, Resources, and Tectonic Evolution. *Geological Society*, London, Memoir, 31. DOI: 10.1017/S0016756806212974

Cameron, N.R., Ghazali, S.A., and Thompson, S.J., 1982. *Geologic Map of The Bengkalis Quadrangle, Sumatra, scale 1:250.000*. Pusat Penelitian dan Pengembangan Geologi, Bandung.

Christiansen, E.H. and Keith, J.D., 1996. Trace element systematics in silicic magmas: a metallogenic perspective. *In*: Trace Element Geochemistry of Volcanic Rocks: Applications for Massive Sulfide Exploration, *Geological Association of Canada, Short Course Notes*, 12, p.115-151.

Cobbing, E.J., Pitfield, P. E. J., Darbyshire, D. P. F., and Mallick, D. I. J., 1992. The granites of the South-East Asian tin belt. *Overseas Memoir*, 10, British Geological Survey. DOI: 10.1144/gsjgs.143.3.0537

Diantoro, S., 2014. The Effect of Implementation of Licencing Policies of Granite Mining to the Effectiveness of Environmental Management in Karimun District of Riau Islands Province. *The International Journal of Social Science*, 22 (1), p.98 - 123.

Djunaedi, E.K., Utoyo, and Sutrisno, 2005. Pemantauan dan Evaluasi Konservasi Sumber Daya Mineral di Daerah Kabupaten Karimun, Provinsi Riau. *Kolokium Hasil Lapangan – DIM 2005*, p.49-1 – 49-10.

Dwivedi, A.K., Pandey, U.K., Bhatt, A.K., Babu, P.V.R., and Joshi, M., 2011. Geochemistry and Geochronology of A-type Barabazar Granite: Implications on the Geodynamics of South Purulia Shear Zone, Singhbhum Craton, Eastern India. *Journal Geological Society of India*, 77, p.527-538. DOI: 10.1007/s12594-011-0055-y

Faure, M., Lepvrier, C., Vuong, N.V., Lin, W. and Chen. Z., 2014. The South China Block-Indochina collision: where, when, and how? *Journal of Southeast Asian earth sciences*, 79, p.260-274. DOI: 10.1016/j.jseaes.2013.09.022

Ghani. A.A., 2005. Highly evolved S type granite: Selim Granite, Main Range Batholith, Peninsular Malaysia. *Geological Society of Malaysia Bulletin*, 51, p.95-101.

Ghani, A.A., Yusoff, I., Hassan, M.H.A., and Ramli, R., 2013. Geochemical study of volcanic and associated granitic rocks from Endau Rompin, Johor, Peninsular Malaysia. *Journal of Earth System Science*, 122 (1), p.65-78. DOI:10.1007/s12040-012-0250-2.

Goodge, J.W. and Vervoot, J.D., 2006. Origin of Mesoproterozoic A-type granites in Laurentia: Hf isotope evidence. *Earth and Planetary Science Letters*, 243, p.711–731. DOI:10.1016/j.epsl.2006.01.040

Irzon, R. and Permanadewi, S., 2010. Elements Study of Igneous and Altered Rocks in Kulonprogo and Its Surrounding Using ICP-MS. *Proceeding PIT IAGI, Lombok*.

Irzon, R., 2015. Contrasting Two Facies of Muncung Granite in Lingga Regency Using Major, Trace, and Rare Earth Element Geochemistry. *Indonesian Journal on Geoscience*, 2 (1), p.23-33. DOI:10.17014/ijog.2.1.23-33.

Jurvanen, T., Eklund, O., and Vaisanen, M., 2005. Generation of A-type granitic melts during the late Svecofennian metamorphism in southern Finland. *GFF*, 127, p.139-147. DOI: 10.1080/11035890501272139

Kebede, T., Koeberl, C., and Koller F., 1999. Geology, Geochemistry and Petrogenesis of Intrusive Rocks of The Wallaga Area, Western Ethiopia. *Journal of African Earth Sciences*, 29 (4), p.715-734. DOI: 10.1016/S0899-5362(99)00126-8

Keshavarzi, R., Esmaili, D., Kahkhaei, M.R., Mokhtari, M.A.A., and Jabari, R., 2014. Petrology, Geochemistry and Tectonomagmatic Setting of Neshveh Intrusion (NW Saveh). *Open Journal of Geology*, 4, p.177-189. DOI:10.4236/ojg.2014.45013.

Kurniawan, A., 2014. Geologi Batuan Granitoid di Indonesia dan Distribusinya. *Masyarakat Ilmu Bumi Indonesia*, 1(E-3), p.1-16.

Mao, J., Xie, G., Duan, C., Pirajno, F., Ishiyama, D., and Chen, Y., 2011. A tectono-genetic model for porphyry–skarn–stratabound Cu–Au–Mo–Fe and magnetite–apatite deposits along the Middle–Lower Yangtze River Valley, Eastern China. *Ore Geology Reviews*, 43, p.294-314. DOI: 10.1016/j.oregeorev.2011.07.010

McDonough, W.F. and Sun, S. 1995. Composition of the Earth. *Chemical Geology*, 120, p.223-253. DOI:10.1016/0009-2541(94)00140-4.

Metcalfe, I., 2000. The Bentong-Raub suture zone. *Journal of Asian Earth Science*, 18, p.691-712. DOI:10.1016/S1367-9120(00)00043-2.

Middlemost, E.A.K., 1985. Naming Materials in the Magma/Igneous Rock System. *Earth-Science Reviews*, 37, p.215-224. DOI:10.1016/0012-8252(94)90029-9.

Nagudi, B., Koeberl, C., and Kurat, G., 2003. Petrography and geochemistry of the Singo granite, Uganda, and implications for its origin. *Journal of African Earth Sciences*, 36, p.73-87. DOI: 10.1016/S0899-5362(03)00014-9

Papangelakis, V.G. and Moldoveanu, G., 2014. Recovery of Rare Earth Elements From Clay Minerals. *ean Rare Earth Resources Conference*, p.191-202.

Peccerillo, R. and Taylor, S.R., 1976. Geochemistry of Eocene calc-alkaline volcanic rocks from the Kastamonu area, Northern Turkey. *Contributions to Mineralogy and Petrology*, 58, p.63-81. DOI:10.1007/BF00384745.

Pulonggono, A. and Cameron, N.R., 1984. Sumatran microplates, their characteristics and their role in the evolution of the Central and South Sumatra basins. *Indonesian Petroleum Association, Proceedings of the 13th Annual Convention*, 13, p.1221 - 1443.

Ray, J., Saha, A., Ganguly, S., Balaram, V., Krishna, A.K., and Hazra, S. 2011. Geochemistry and petrogenesis of Neoproterozoic Mylliem granitoids, Meghalaya Plateau, northeastern India. *Journal of Earth System Science*, 120 (3), p.459-473. DOI:10.1007/s12040-011-0084-3.

Sahoo, S.K., Hosoda, M., Kamagata, S., Sorimachi, A., Ishikawa, T., Tokonami, S., and Uchida, S., 2011. Thorium, Uranium and Rare Earth Elements Concentration in Weathered Japanese Soil Samples. *Progress in Nuclear Science and Technology*, 1, p.416-419.

Salem, L.A., Abdel-Moneum, A.A., Shazly, A.G., and El-Shibiny, N.H., 2001. Mineralogy and geochemistry of Gabal El-lneigi Granite and associated fluorite veins, Central Eastern Desert, Egypt: application of fluid inclusions to fluorite genesis. *Journal of African Earth Sciences*, 32(1), p. 29-45. DOI: 10.1016/S0899-5362(01)90017-X

Shand, S.J., 1943. *Eruptive rocks*. D. Van Nostrand Company, New York, 360pp.

Shellnutt, J.G. and Zhou, M.F., 2007. Permian peralkaline, peraluminous and metaluminous A-type granites in the Panxi district, SW China: Their relationship to the Emeishan mantle plume. *Chemical Geology*, 243, p.286–316. DOI:10.1016/j.chemgeo. 2007.05.022.

Singh, L.S. and Vallinayagam, G., 2012. High Heat Producing Volcano-Plutonic Rocks of the Siner Area, Malani Igneous Suite, Western Rajasthan, India. *International Journal of Geosciences*, 3, p.1137-1141. DOI: 10.4236/ijg.2012.35115.

Sone, M. and Metcalfe, I., 2008. Parallel Tethyan sutures in mainland Southeast Asia: New insights for Palaeo-Tethys closure and implications for the Indosinian orogeny. *Comptes Rendus Geoscience*, 340, p.166-179. DOI: 10.1016/j.crte.2007.09.008

Streckeisen, A., 1976. To each plutonic rock its proper name. *Earth-Science Reviews*, 12, p.1–33.

Tong Y., Wang, T., Siebel, W., Hong, D.W., and Sun, M., 2012. Recognition of early Carboniferous alkaline granite in the southern Altai orogen: post-orogenic processes constrained by U–Pb zircon ages, Nd isotopes, and geochemical data. *International Journal of Earth Science (Geologische Rundschau)*, 101, p.937–950. DOI: 10.1007/s00531-011-0700-0.

Warith, A.A., Michalik, M., and Ali, B.H., 2010. Luorine Enriched Granites: Chemical

Characterization and Relation to Uranium Mineralization. *Journal of Applied Sciences Research*, 6(4), p.299-323 ?

Whalen, J. B., Currie, K. L., and Chappell, B. W., 1987. A-type granites: Geochemical characteristics, discrimination and petrogenesis. *Contributions to Mineralogy and Petrology*, 96, p.407-419. DOI: 10.1007/BF00402202

White, W.M., 2013. *Geochemistry*. Wiley-Blackwell, UK. 668pp. DOI: 10.1017/S0016756813000708

Zhang, J., Ma, C. and She, Z., 2012. An Early Cretaceous garnet-bearing metaluminous A-type granite intrusion in the East Qinling Orogen, central China: Petrological, mineralogical and geochemical constraints. Geoscience Frontiers, 3 (5), p.635-646. DOI: 10.1016/j.gsf.2011.11.011